The calcimimetic etelcalcetide attenuates pressure overload-induced cardiac hypertrophy in rats with and without chronic kidney disease

Okamoto, Hidehisa
Goto, Shunsuke
Nose, Yuma
Okamoto, Hayaki
Fujii, Hideki

(Citation)
Biomedicine & Pharmacotherapy,196:119054

(Issue Date)
2026-03

(Resource Type)
journal article

(Version)
Version of Record

Biomedicine & Pharmacotherapy 196 (2026) 119054

Contents lists available at ScienceDirect

Biomedicine & Pharmacotherapy

journal homepage: www.elsevier.com/locate/biopha

The calcimimetic etelcalcetide attenuates pressure overload–induced cardiac hypertrophy in rats with and without chronic kidney disease

Hidehisa Okamoto, Shunsuke Goto, Yuma Nose, Hayaki Okamoto, Hideki Fujii *

Division of Nephrology, Kobe University Graduate School of Medicine, Kobe, Japan

ARTICLE INFO

Keywords:
Calcimimetics
Calcium-sensing receptor
Cardiac hypertrophy
Chronic kidney disease
Renin-angiotensin-aldosterone system

ABSTRACT

Introduction: Calcimimetics such as etelcalcetide (ET) are used to manage secondary hyperparathyroidism patients with chronic kidney disease (CKD) on dialysis. While their cardiovascular benefits—including left ventricular hypertrophy (LVH) suppression—are recognized, the underlying mechanisms remain unclear. This study investigated how ET suppresses LVH using rat models.

Methods: LVH was induced via transverse aortic coarctation, and CKD by 5/6 nephrectomy. Rats were assigned to the sham, CKD, LVH, or CKD/LVH groups, with each pathological group further divided into vehicle- or ET-treated subgroups. After eight weeks of treatment, echocardiography, histological, biochemical, and molecular analyses were conducted.

Results: ET reduced serum parathyroid hormone and fibroblast growth factor 23 (FGF23) levels in the CKD and CKD/LVH groups but not in the LVH group, where these levels were not increased. ET did not affect serum calcium, phosphorus, or vitamin D levels in the LVH and CKD/LVH groups. Nonetheless, ET suppressed cardiac hypertrophy and cardiomyocyte enlargement in the LVH and CKD/LVH groups despite no changes in systemic mineral metabolism parameters. Mechanistically, ET attenuated cardiac hypertrophy, serum aldosterone levels, and cardiac renin-angiotensin-aldosterone system (RAAS) components in the LVH and CKD/LVH groups. Cardiac FGF23 expression, elevated in the LVH and CKD/LVH groups, was also decreased by ET. The calcineurin/nuclear factor of the activated T-cell signaling pathway was unaffected.

Conclusion: ET effectively suppressed LVH in the LVH and CKD/LVH groups. These findings suggest that ET's cardioprotective effects are mediated via the modulation of the RAAS and cardiac FGF23 expression rather than solely through the correction of CKD-mineral bone disorder abnormalities.

1. Introduction

The leading cause of death in patients with chronic kidney disease (CKD) is cardiovascular disease (CVD) [1]. Left ventricular hypertrophy (LVH), a cardiac structural abnormality [2], is associated with CVD pathogenesis [3], and patients with CKD have a high prevalence of LVH [4]. According to a previous study, even in the early stages of CKD (stage 1–2), 51 % of patients exhibit LVH, increasing to 78 % in CKD stages 3–5 [5]. Furthermore, LVH has been identified as a significant risk factor for CVD not only in patients without CKD but also in patients with CKD. Although the progression of CVD has been reported to involve multiple contributing factors, including hemodynamic stress, neuroendocrine activation, and metabolic abnormalities [2,5,6], the underlying pathophysiology remains complex and incompletely understood.

The mechanisms underlying LVH progression in CKD include hypertension, volume overload, activation of the renin-angiotensin-aldosterone system (RAAS), anemia, and diabetes [1,4,7]. Among them, CKD-mineral bone disorder (CKD-MBD) has also been identified as critical [8]. A significant correlation between parathyroid hormone (PTH) levels and LVH has been demonstrated [9]. Elevated PTH activates pathways such as protein kinase C (PKC) and transforming growth factor-beta 1 (TGF-β1), promoting LVH progression [10]. Additionally, elevated serum phosphate levels independently contribute to LVH progression, separate from PTH elevation [11]. The phosphaturic hormone fibroblast growth factor 23 (FGF23) also has been implicated in LVH progression in clinical and basic research studies [12,13]. Furthermore, Klotho—another key factor—has also been reported to play a role in LVH pathogenesis [14]. LVH improvement has been reported to potentially mitigate the risks of all-cause and cardiovascular mortality in patients with CKD [15]. Thus, addressing LVH in patients with CKD is

* Correspondence to: Division of Nephrology, Kobe University Graduate School of Medicine, 7-5-2, Kusunoki-cho, Chuo-ku, Kobe, Hyogo 650-0017, Japan.
E-mail address: fhideki@med.kobe-u.ac.jp (H. Fujii).

https://doi.org/10.1016/j.biopha.2026.119054
Received 21 October 2025; Received in revised form 17 January 2026; Accepted 21 January 2026
Available online 30 January 2026

considered crucial; however, effective treatment options for this are not yet fully established.

Active vitamin D deficiency has been implicated in LVH progression, and vitamin D analogs have been reported in both basic and observational clinical studies to inhibit LVH progression [16–18]. Unfortunately, several randomized controlled trials could not prove the efficacy of these treatments [19,20].

In recent years, calcium-sensing receptor (CaSR) agonists, widely used as therapeutic agents for CKD-MBD, have been shown to reduce not only PTH but also FGF23 levels [21]. This dual effect has raised expectations for their potential to suppress cardiac hypertrophy. Indeed, some studies have demonstrated that CaSR agonists improve LVH [22,23] and suppress heart failure onset [24]. Thus, CaSR agonists are considered to potentially exert beneficial effects on the heart; however, the underlying mechanisms remain insufficiently understood. Therefore, this study aimed to investigate the effects of a CaSR agonist, etelcalcetide (ET), on LVH and elucidate its pharmacological mechanisms using CKD and pressure overload-induced LVH model rats.

2. Materials and methods

2.1. Animals

We purchased Male Sprague-Dawley (SD) rats from SLC Japan Inc. These rats were housed under controlled light and temperature conditions, with free access to food and water. At 8 weeks of age, the rats were randomly divided into seven groups as follows: sham-operated rats treated with vehicle (sham, n=6), CKD-induced rats treated with vehicle (CKD, n=6), CKD-induced rats treated with ET (CKD+ET, n=6), LVH-induced rats treated with vehicle (LVH, n=6), LVH-induced rats treated with ET (LVH+ET, n=6), CKD- and LVH-induced rats treated with vehicle (CKD/LVH, n=6), and CKD- and LVH-induced rats treated with ET (CKD/LVH+ET, n=6). All groups were fed a high-phosphate diets containing 1.0 % calcium and 1.2 % phosphate. At 8 weeks of age, transverse aortic constriction (TAC) was performed on rats in the LVH and CKD/LVH groups. Briefly, anesthesia was induced with isoflurane, followed a mixture of medetomidine, midazolam, and butorphanol was administered intraperitoneally. The rats underwent tracheal intubation using 17-gauge vascular catheters and were mechanically ventilated with a small animal ventilator (MK-V100, Muromachi Kikai). After thoracotomy, a 5–0 silk suture was placed around the transverse aorta between the innominate artery and the left common carotid artery. The aorta was constricted by tying the suture firmly around it with a 25-gauge needle positioned as a spacer. At 9 weeks of age, a left two-thirds nephrectomy was performed on the CKD and CKD/LVH groups, followed by a right nephrectomy at 10 weeks of age. Sham operations were performed on rats in the sham group at the corresponding ages (8, 9, and 10 weeks).

Treatment with vehicle or ET began at 11 weeks of age and continued daily until sacrifice at 19 weeks of age (Fig. 1). ET was administered subcutaneously at a dose of 0.5 mg/kg/day. The 24-hour urine was collected from each rat housed individually in metabolic cages, and echocardiographic parameters were measured prior to euthanasia at 19 weeks of age. Blood samples for serum analysis were collected from the left ventricle, and the hearts were harvested for RNA and protein extraction, as well as histomorphological analysis.

All procedures were performed in accordance with the National Institutes of Health Guide for the Care and Use of Laboratory Animals. The experimental protocol was approved by the Ethics Committee of the Animal Experiment Facility at the Kobe University Graduate School of Medicine (Permit No.: P190795-R1). All surgical procedures were carried out under anesthesia using 1.5 % isoflurane, supplemented with intraperitoneal premedications of midazolam (2 mg/kg), medetomidine (0.375 mg/kg), and butorphanol (2.5 mg/kg). All efforts were made to minimize animal suffering, in accordance with the Animal Research: Reporting of In Vivo Experiments (ARRIVE) guidelines for reporting animal research [25].

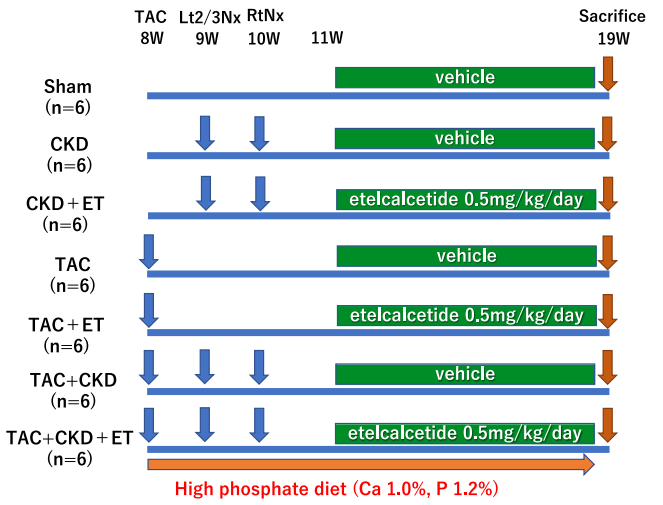

Fig. 1. Protocol of the experiments.

2.2. Biochemical analysis

Blood and urine samples were centrifuged at 3000 rpm for 10 min, and the supernatants were stored at −80°C until analysis. Serum levels of blood urea nitrogen and creatinine were measured using the Fuji Dri-Chem 3500 system (FUJIFILM, Tokyo, Japan). Serum calcium, phosphorus, and urinary creatinine levels were measured using the Calcium E-Test Wako, Phospha C-Test Wako, and LabAssay Creatinine kits (FUJIFILM Wako Pure Chemical Industries, Osaka, Japan), respectively. Serum 1,25$(OH)_2$ vitamin D and 25(OH) vitamin D levels were analyzed by SRL Inc. (Tokyo, Japan). Serum intact parathyroid hormone (iPTH) levels were quantified using Rat Bioactive intact PTH ELISA kit (Quidel Corporation, San Diego, CA, USA). Serum intact fibroblast growth factor 23 (iFGF23) levels were measured using FGF23 ELISA kit (KAINOS laboratories, Inc., Tokyo, Japan). Serum aldosterone, and urinary 8-hydroxy-2'-deoxyguanosine (8-OHdG) levels were quantified using Aldosterone ELISA kit (Abcam, Cambridge, UK) and 8-OHdG ELISA kit (KOG-200SE, Japan Institute for the Control of Aging, Shizuoka, Japan), respectively.

2.3. Blood pressure measurement

Tail-cuff plethysmography (MK-2000; Muromachi Kikai Co., Ltd., Tokyo, Japan) was used for the measurement of systolic blood pressure. To minimize stress-induced hypertension, rats were allowed to acclimatize to the testing environment for no less than 15 min prior to blood pressure measurement. A total of 10 readings were taken and averaged to obtain the final value.

2.4. Echocardiographic measurements

Transthoracic echocardiography (F37 and UST-5299 ultrasound transducer probe; Hitachi Aloka Medical, Ltd., Tokyo, Japan) was performed under 1.5 % isoflurane anesthesia. A two-dimensional short-axis image of the left ventricle was obtained at the level of the papillary muscles.

2.5. Histological and immunohistochemical analysis

Hearts were excised, fixed in 10 % formaldehyde, and embedded in paraffin blocks. Sections from the paraffin blocks were stained with Sirius Red for morphometric measurements. The remaining heart tissue was embedded in OCT compound, frozen, and cryosectioned. These

cryosections were stained with Alexa Fluor 488-labeled wheat germ agglutinin (WGA; Thermo Fisher Scientific, Carlsbad, CA, USA; W11261) according to the protocol provided by the manufacturer. The percentage of positive regions in Sirius Red staining and the cross-sectional area of myocardial fibers in WGA staining were analyzed using image analysis software (imageJ, National Institutes of Health, USA).

Immunohistochemical staining was performed to evaluate the expression of angiotensin-converting enzyme (ACE), ACE2, angiotensin II (Ang ll), FGF23 and calcium-sensing receptor (CaSR). The following primary antibodies were used: anti-ACE antibody (SantaCruz Biotechnology, Inc., CA, USA; sc-23908), anti-ACE2 antibody (Abcam, Cambridge, UK; ab108252), anti-Ang II antibody (Novus Biologicals, Littleton, CO, USA; NB100–62346), anti-FGF23 antibody (MybioSource, Inc, San Diego, CA, USA; MBS854462), anti-CaSR antibody (Life Technology, Carlsbad, CA, USA; MA1–934), and anti-8-OHdG monoclonal antibody (Japan Institute for the Control of Aging, Shizuoka, Japan; MOG-020P). The sections were incubated with the primary antibodies for 60 min at room temperature (ACE2 and CaSR) or overnight at 4°C (ACE, Ang II, FGF23, and 8-OHdG). For the immunohistochemistry of ACE, ACE2, Ang II, and FGF23, a universal immunoperoxidase polymer (Nichirei Biosciences Inc., Tokyo, Japan; NIC-414191F) was used. For 8-OHdG, a biotinylated anti-mouse immunoglobulin G secondary antibody (Vector Laboratories, Newark, CA, USA; BA-2000) was applied, followed by detection using the ABC reagent (Vector Laboratories, Newark, CA, USA; PK-6100). In all immunohistochemical procedures, color development was achieved using 3,3′-diaminobenzidine as the chromogenic substrate.

The regions with positive immunohistochemical staining were quantified using ImageJ software. The number of 8-OHdG-positive cells was expressed as the number of positive cells per 0.01 mm^2 of the analyzed area.

2.6. RNA extraction and real-time polymerase chain reaction

Total RNA was extracted from frozen heart tissues using RNAiso Plus (Takara Bio Inc., Shiga, Japan), and complementary DNA was synthesized using the ReveTra ACE qPCR RT Kit (TOYOBO Co., Ltd., Osaka, Japan). Real-time polymerase chain reaction (RT-PCR) was conducted using a SYBR Green assay on the Applied Biosystems 7500 real-time PCR system (Thermo Fisher Scientific, Waltham, MA, USA) with Thunderbird SYBR qPCR Mix (TOYOBO Co., Ltd., Osaka, Japan). Quantitative analysis of mRNA expression was conducted using the relative quantification algorithm implemented in the Applied Biosystems 7500 Real-Time PCR Software. Target gene expression was normalized to GAPDH, which served as the reference gene. The primer sequences used for amplification were as follows: GAPDH: forward 5′-TGGGAAGCTGGTCATCAAC-3′, reverse 5′-GCATCACCCCATTTGATGTT-3′; FGF23; forward 5′-TTGG ATCGTATCACTTCAGC-3′, reverse 5′-TGCTTCGGTGACAGGTAG-3′; α-m yosin heavy chain (α-MHC): forward 5′-GAGCAGGAGCTGATCGAGAC-3′, reverse 5′-CCTCTGCGTTCCTACACTCC-3′; β-myosin heavy chain (β-M HC): forward 5′-CTCCAGAAGAGAAGAACTCC-3′, reverse 5′-CCACCTGC TGGACATTCTGC-3′; atrial natriuretic peptide (ANP): forward 5′-AGG-CAGTCGATTCTGCTTGA-3′, reverse 5′-CGTGATAGATGAAGGCAGGAA G-3′; brain natriuretic peptide (BNP): forward 5′-CCAGAACAATC CACGATGC-3′, reverse 5′-TCGAAGTCTCTCCTGGATCC-3′; angiotensinogen (AGT): forward 5′-TTGTGTGAGGAGGGCTGTAT-3′, reverse 5′-TGCTGAGAGTGTAGGTCCTG-3′; angiotensin II type 1 receptor (AT1R): forward 5′-CTCAAGCCTGTCTACGAAAATGAG-3′, reverse 5′-GTGAATG GTCCTTGGTCGT-3′; angiotensin l converting enzyme (ACE): forward 5′-TGCCTAGATCCCAAGGTGAC-3′, reverse 5′-CAACTTCATGGCATCTGC-CAGCA-3′; angiotensin l converting enzyme 2 (ACE2): forward 5′-CCCAGAGAACAGTGGACCAAAA-3′, reverse 5′-GCTCCACCACACCAAC GAT-3′; renin: forward 5′-CTGTGCATACTGGCTCTCCA-3′, reverse 5′-GGCTTGGCCTAAAACTAGGG-3′; connective tissue growth factor (CTGF): forward 5′-GCGGCGAGTCCTTCCAA-3′, reverse 5′-CCACG GCCCCATCCA-3′; CaSR: forward 5′-TGACGAGCCTCAGAAGAATGC-3′, reverse 5′-CCTCCACCACTAATGACGAAGC-3′; sarcoplasmic/endoplas mic reticulum Ca^{2+} ATPase 2a (SERCA2a): forward 5′-CTGGCCGAC-GACAACTTCTC-3′, reverse 5′-TGAGGTAGCGGATGAACTGCTT-3′; rya-nodine receptor 2 (RyR2): forward 5′-TGCTGCGAGCCGGG-3′, reverse 5′-TGGCGGTGGCGTAGGA-3′; protein phosphatase 3 catalytic subunit alpha (Ppp3ca): forward 5′-TGCAAAGCGCTACTGTTGAG-3′, reverse 5′-GCTGTCTGTGCCGTTAGTCT-3′; regular of calcineurin 1 (Rcan1); forward 5′-TTGGGAACTGTTGGTTGACA-3′, reverse 5′-ATGGCTACGGCA-TACTCCAC-3′.

2.7. Protein extraction and western blot analysis

Frozen heart samples were homogenized in PRO-PREP (Cosmo Bio Co., Ltd., Tokyo, Japan), a protein extraction reagent, supplemented with PhosSTOP (Roche Diagnostics, Mannheim, Germany), a phosphatase inhibitor. After centrifugation at 13,000 rpm for 5 min, the supernatant of the homogenate was collected to obtain the lysate. The lysate was mixed with LDS Sample Buffer (4x) and Reducing Agent (10x) (Thermo Fisher Scientific, Waltham, MA, USA), followed by heat treatment at 70°C for 10 min. Protein was separated by SDS-PAGE using Tris-based Mini Protein Gels (Thermo Fisher Scientific, Waltham, MA, USA) and transferred onto PVDF membrane (Bio-Rad, Richmond, CA, USA) via electroblotting. The membranes were blocked with either TBS-T (150 mM NaCl, 50 mM Tris-HCl and 0.05 % Tween 20) containing 5 % skimmed milk or Blocking One-P (Nacalai Tesque, Inc., Kyoto, Japan). The following primary antibodies were used for incubation: anti-β-actin antibody (SantaCruz Biotechnology, Inc., CA, USA; sc-47778), anti-NFAT (nuclear factor of the activated T-cell) c4 antibody (SantaCruz Biotechnology, Inc., CA, USA; sc-271597), and anti-p-NFATc4 antibody (SantaCruz Biotechnology, Inc., CA, USA; sc-135771). After incubation with the primary antibody for 30 min at room temperature or overnight at 4°C, the membrane was washed and then incubated with the secondary antibody, m-IgGκ BP-HRP (SantaCruz Biotechnology, Inc, CA, USA; sc-516102), for 30 min at room temperature. Protein signals ware visualized using the chemiluminescent reagent Chemi-Lumi super one (Nacalai tesque, Kyoto, Japan) and captured with the Amersham Imager 600 (GE Healthcare Bioscience, Piscataway, NJ, USA). Results were analyzed using image analysis software (ImageJ, National Institutes of Health, USA).

2.8. Statistical analysis

All statistical analyses were performed using IBM SPSS statistics software version 29.0 (IBM Corp., Armonk, NY, USA). All data are expressed as the mean ± standard error. To evaluate the effects of ET in the CKD, LVH, and CKD/LVH groups, data were analyzed using a two-way analysis of variance (ANOVA) with group (CKD, LVH, CKD/LVH) and treatment (vehicle vs. ET) as factors. When a significant interaction was detected, simple effects were examined by comparing the vehicle- and ET-treated rats within each group, with adjustment for multiple comparisons using the Sidak method. Comparisons among the vehicle-treated sham, CKD, LVH, and CKD/LVH groups were performed using one-way ANOVA followed by Dunnett's test, with the sham group as the reference. A *P*-value of less than 0.05 was considered statistically significant.

3. Results

3.1. Animal characteristics and biochemical data

Table 1 summarizes the characteristics and biochemical parameters of the rats at 19 weeks of age. Among the groups, blood pressure was higher in the CKD group than in the sham group, whereas no significant differences were observed between the LVH or CKD/LVH groups and the sham group. Heart rate was comparable across all groups. Serum blood

Table 1
Animal characteristics at 19 weeks.

	Sham N = 6	CKD N = 6	CKD + ET N = 6	LVH N = 6	LVH + ET N = 6	CKD/LVH N = 6	CKD/LVH + ET N = 6
BW (g)	524.8 ± 13.4	445.2 ± 8.2#	442.2 ± 12.7	461.0 ± 18.5	526.3 ± 13.3	439.3 ± 27.9#	458.2 ± 8.8
sBP (mmHg)	117.4 ± 0.9	126.9 ± 0.8#	125.0 ± 2.1	119.2 ± 2.4	119.7 ± 1.6	119.7 ± 1.3	118.0 ± 2.8
HR (/min)	448.3 ± 10.0	475.4 ± 11.9	446.8 ± 11.9	436.7 ± 18.3	419.3 ± 15.8	433.5 ± 9.0	428.2 ± 10.7
BUN (mg/dL)	13.1 ± 1.3	29.6 ± 1.8#	28.4 ± 1.9	14.5 ± 0.8	15.1 ± 0.5	30.5 ± 2.4#	30.3 ± 1.7
Cr (mg/dL)	0.26 ± 0.01	0.70 ± 0.04#	0.70 ± 0.05	0.28 ± 0.01	0.28 ± 0.01	0.76 ± 0.05#	0.62 ± 0.04
Ca (mg/dL)	10.5 ± 0.2	9.1 ± 0.1#	8.5 ± 0.3a	10.3 ± 0.2	10.1 ± 0.2	9.2 ± 0.1#	8.9 ± 0.2
P (mg/dL)	6.8 ± 0.3	9.4 ± 0.4#	9.3 ± 0.5	7.1 ± 0.3	7.1 ± 0.2	9.6 ± 0.3#	10.0 ± 0.5
1.25(OH)$_2$VitD (pg/mL)	363.2 ± 28.2	291.2 ± 30.8	289.5 ± 11.1	315.7 ± 23.9	352.3 ± 17.1	222.7 ± 4.1#	269.3 ± 21.5
25(OH)VitD (pg/mL)	43.7 ± 1.5	42.5 ± 3.2	44.3 ± 3.1	47.2 ± 3.4	44.3 ± 1.6	44.0 ± 1.6	41.8 ± 5.5

Abbreviations: CKD, chronic kidney disease; LVH, left ventricular hypertrophy; ET, etelcalcetide; BW, Body Weight; sBP, systolic blood pressure; HR, heart rate; BUN, blood urea nitrogen; Cr, creatinine; Ca, calcium; P, phosphate; 1,25(OH)$_2$VitD, 1,25-dihydroxyvitamin D; 25(OH)VitD, 25-hydroxyvitamin D.
#; P < 0.05, vs. sham group, a; P < 0.05, CKD group vs. CKD + etelcalcetide (ET) group, b; P < 0.05, LVH group vs. LVH + ET group, c; P < 0.05, vs. CKD/LVH group vs. CKD/LVH + ET group.

urea nitrogen (BUN) and creatinine (Cr) levels were elevated in the CKD and CKD/LVH groups compared to the sham group, while these levels in the LVH group were similar to those in the sham group. Furthermore, ET did not significantly affect blood pressure, heart rate, BUN, or Cr levels in any group.

3.2. Echocardiographic parameters and cardiac weight

The echocardiographic parameters and heart weight at 19 weeks of age are shown in Table 2. Significant increments in interventricular septal thickness at end-diastole and left ventricular posterior wall thickness in diastole were observed in the LVH and CKD/LVH groups. Treatment with ET significantly suppressed these increments in the CKD/LVH group. Additionally, the CKD, LVH, and CKD/LVH groups showed significant reductions in the left ventricular ejection fraction and fractional shortening, both of which were significantly attenuated with ET in the LVH and CKD/LVH groups. The heart weight-to-body weight ratio was also significantly elevated in the LVH and CKD/LVH groups. ET treatment tended to attenuate this ratio in the LVH group and significantly attenuated it in the CKD/LVH groups.

3.3. Assessment of cardiac hypertrophy and fibrosis

In WGA-stained myocardial tissue, the cardiomyocyte area was significantly increased in the LVH and CKD/LVH groups (Fig. 2a), and ET significantly attenuated cardiomyocyte hypertrophy in both groups.

In the LVH and CKD/LVH groups, myocardial mRNA expression levels of ANP, BNP, and β-MHC were significantly elevated, while α-MHC expression was significantly reduced (Fig. 2b, c, d, and e). ET treatment led to significant improvements in these expression levels.

Cardiac fibrosis (assessed using Sirius Red staining) was significantly worsened in the LVH and CKD/LVH groups (Fig. 3a). ET treatment significantly prevented cardiac fibrosis in both groups. Additionally, in the CKD/LVH group, myocardial mRNA expression of CTGF was significantly increased; however, ET treatment significantly reduced its expression (Fig. 3b).

3.4. CKD-MBD-related parameters in the serum and heart

No significant differences in serum phosphate, 1,25(OH)$_2$ vitamin D~~,~~ and 25(OH) vitamin D levels were observed between the vehicle- and ET-treated groups across the CKD, LVH, and CKD/LVH groups. Serum calcium levels were suppressed in the CKD group and tended to be lower in ET-treated rats than in the vehicle-treated rats in the CKD/LVH group (Table 1).

As shown in Fig. 4a, serum intact PTH levels were elevated in the CKD and CKD/LVH groups compared to the sham group. Treatment with ET suppressed the elevation of serum intact PTH levels significantly in the CKD/LVH group and tended to suppress them in the CKD group. Similarly, serum intact FGF23 levels were elevated in the CKD and CKD/LVH groups compared to the sham group, and ET treatment significantly suppressed these levels in the CKD and CKD/LVH groups (Fig. 4b). In the LVH group, neither serum intact PTH nor serum intact FGF23 levels were elevated, and no changes were observed with ET treatment.

Cardiac mRNA expression of FGF23 was significantly elevated in the CKD/LVH group, and ET treatment significantly reduced its expression in the ~~LVH and~~ CKD/LVH group~~s~~ (Fig. 4c). Immunohistochemical analyses revealed that cardiac expression of FGF23 significantly increased in the LVH and CKD/LVH groups and significantly decreased by ET treatment in both groups (Fig. 4d).

Table 2
Results of the echocardiogram at 19 weeks and heart weight/body weight ratio at the time of sacrifice.

	Sham N = 6	CKD N = 6	CKD + ET N = 6	LVH N = 6	LVH + ET N = 6	CKD/LVH N = 6	CKD/LVH + ET N = 6
LVDd (mm)	7.95 ± 0.07	8.43 ± 0.17	8.50 ± 0.13	8.15 ± 0.20	8.22 ± 0.15	9.03 ± 0.26#	8.52 ± 0.16
LVDs (mm)	4.65 ± 0.03	5.23 ± 0.10#	5.13 ± 0.10	5.67 ± 0.11#	5.28 ± 0.13b	6.77 ± 0.16#	5.65 ± 0.10c
IVSTd (mm)	1.65 ± 0.05	1.77 ± 0.05	1.72 ± 0.05	2.03 ± 0.03#	1.92 ± 0.08	2.25 ± 0.07#	1.92 ± 0.05c
LVPWd (mm)	1.73 ± 0.02	1.83 ± 0.05	1.75 ± 0.04	2.03 ± 0.04#	1.88 ± 0.06	2.33 ± 0.10#	2.08 ± 0.03c
EF (%)	80.0 ± 0.5	76.1 ± 0.4#	78.0 ± 0.5	66.3 ± 0.9#	73.1 ± 1.9b	57.7 ± 1.7#	70.6 ± 1.9c
FS (%)	41.5 ± 0.5	38.2 ± 0.6#	39.7 ± 0.5	30.4 ± 0.7#	35.7 ± 1.5b	25.0 ± 1.1#	33.6 ± 1.4c
HW/BW	2.38 ± 0.07	3.03 ± 0.03	2.81 ± 0.04	3.59 ± 0.08#	3.10 ± 0.07	5.72 ± 0.49#	3.55 ± 0.07c

Abbreviations: CKD, chronic kidney disease; LVH, left ventricular hypertrophy; ET, etelcalcetide; LVDd, left ventricular diastolic diameter; LVDs, left ventricular systolic diameter; IVSTd, interventricular septal thickness at end-diastole; LVPWd, left ventricular posterior wall thickness in diastole; EF, ejection fraction; FS, fractional shortening; HW/BW. Heart weight/Body weight.
#; P < 0.05, vs. sham group, a; P < 0.05, CKD group vs. CKD + etelcalcetide (ET) group, b; P < 0.05, LVH group vs. LVH + ET group, c; P < 0.05, vs. CKD/LVH group vs. CKD/LVH + ET group.

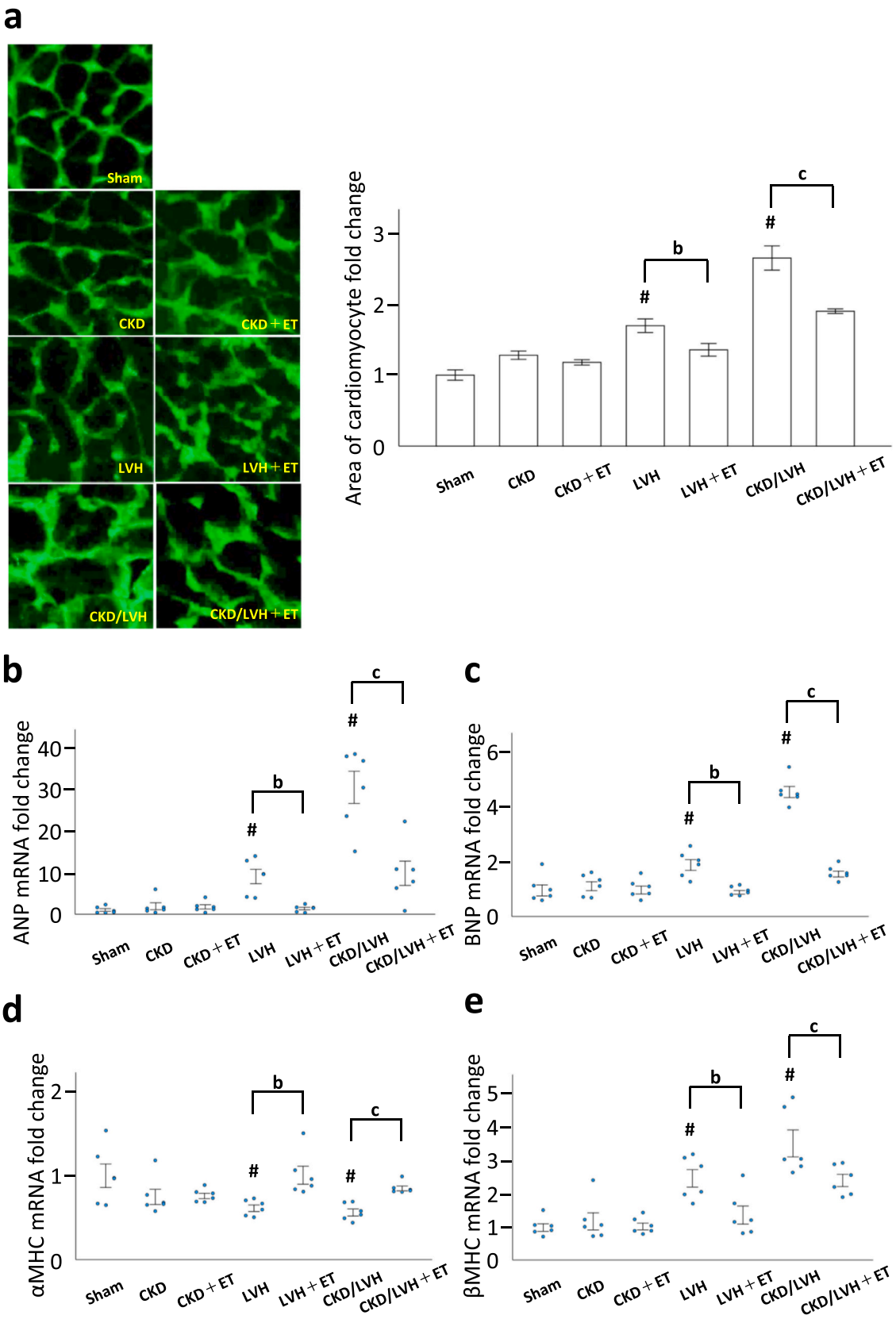

Fig. 2. Evaluation of myocardial hypertrophy. (a) Histological analysis of the cardiomyocyte cross-sectional area using wheat germ agglutinin (WGA) staining. (b) Cardiac mRNA expression of atrial natriuretic peptide (ANP). (c) Cardiac mRNA expression of brain natriuretic peptide (BNP). (d) Cardiac mRNA expression of α-myosin heavy chain (α-MHC). (e) Cardiac mRNA expression of β-myosin heavy chain (β-MHC). Data are presented as the mean ± SEM. #: $P < 0.05$ vs. Sham group; a: $P < 0.05$, CKD group vs. CKD + etelcalcetide (ET) group; b: $P < 0.05$, LVH group vs. LVH + ET group; c: $P < 0.05$, CKD/LVH group vs. CKD/LVH + ET group.

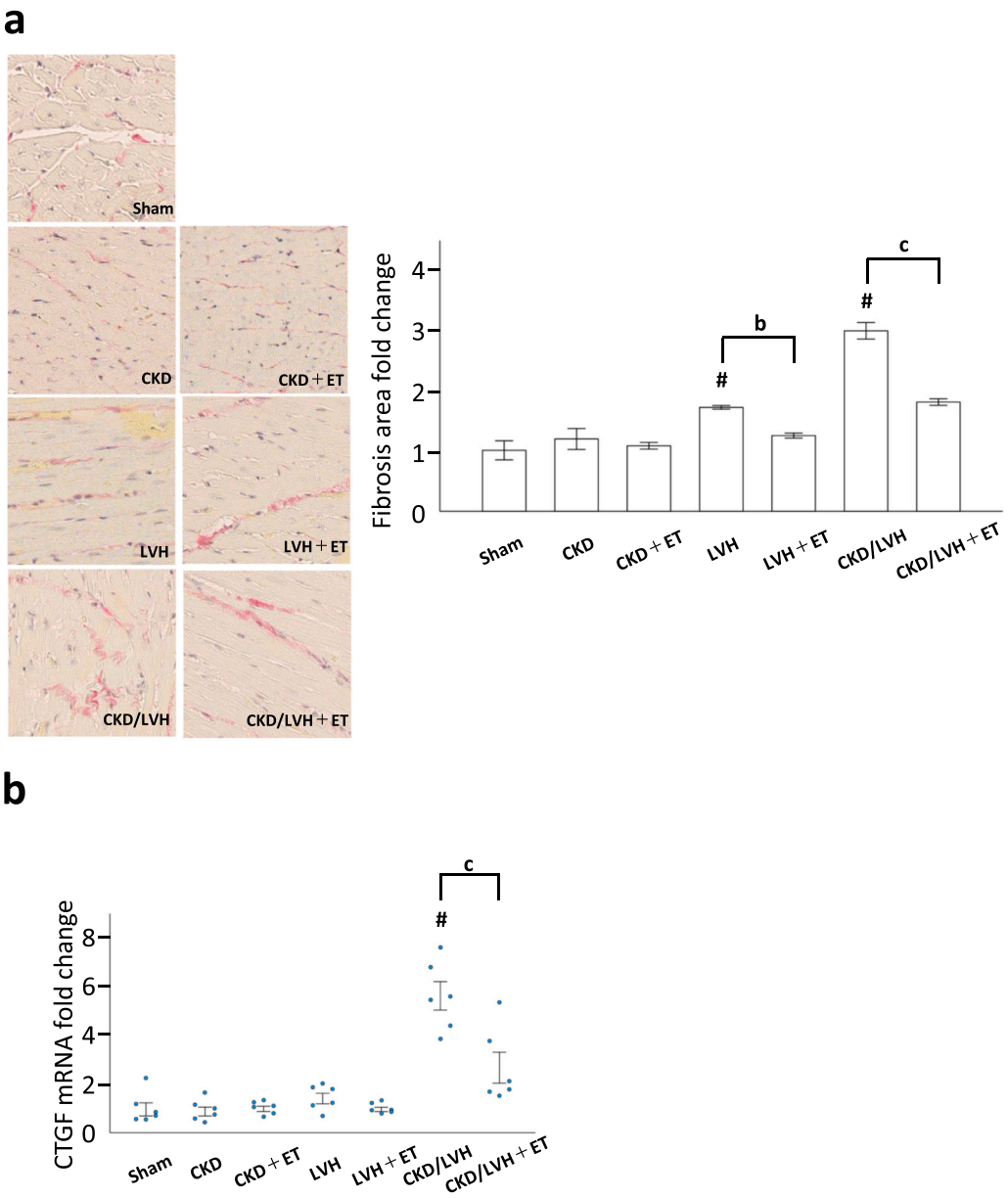

Fig. 3. Evaluation of myocardial fibrosis. (a) Histological assessment of myocardial fibrosis using Sirius Red staining. (b) Cardiac mRNA expression of connective tissue growth factor (CTGF). Data are presented as the mean ± SEM. #: $P < 0.05$ vs. Sham group; a: $P < 0.05$, CKD group vs. CKD + Etelecalcetide (ET) group; b: $P < 0.05$, LVH group vs. LVH + ET group; c: $P < 0.05$, CKD/LVH group vs. CKD/LVH + ET group.

3.5. Evaluation of the CaSR, CaN-NFAT signaling pathway and intercellular calcium regulators in the heart

The mRNA expression of cardiac CaSR was significantly elevated in the CKD, LVH, and CKD/LVH groups (Fig. 5a). ET treatment significantly reduced its expression in the CKD, LVH, and CKD/LVH groups. Immunohistochemical analyses further confirmed that cardiac CaSR expression was significantly increased in the LVH and CKD/LVH groups, and ET treatment led to a significant decrease in CaSR expression in the LVH and CKD/LVH groups (Fig. 5b). Additionally, the mRNA expression levels of SERCA2a and RyR2—intracellular calcium regulators—were evaluated. There were no statistically significant differences among the groups (Fig. 6a and b).

To assess ET's impact on the cardiac calcineurin (CaN)-NFAT signaling pathway, the expression of the pathway-related factors in the heart was evaluated. The mRNA expression levels of Ppp3ca, a subunit of calcineurin Aα, and Rcan1, regulators of the CaN-NFAT pathway, were significantly elevated in the CKD/LVH group. However, ET treatment did not significantly change these expressions (Fig. 6c and d).

In terms of NFAT dephosphorylation, as indicated by the p-NFATc4/NFATc4 ratio, significant reductions were observed in the LVH and CKD/LVH groups. However, no significant changes were detected following ET treatment (Fig. 6e).

3.6. Serum aldosterone and cardiac expressions of RAAS-related factors

Serum aldosterone levels were significantly elevated in the LVH and CKD/LVH groups. ET significantly reduced aldosterone levels in the LVH and CKD/LVH groups (Fig. 7a).

The mRNA expression of cardiac ACE was significantly increased in the CKD/LVH group; however, ET significantly suppressed its expression in the LVH and CKD/LVH groups (Fig. 7b). Furthermore, the mRNA expression of cardiac AGT was significantly increased in the LVH and CKD/LVH groups, and ET significantly suppressed its expression in both

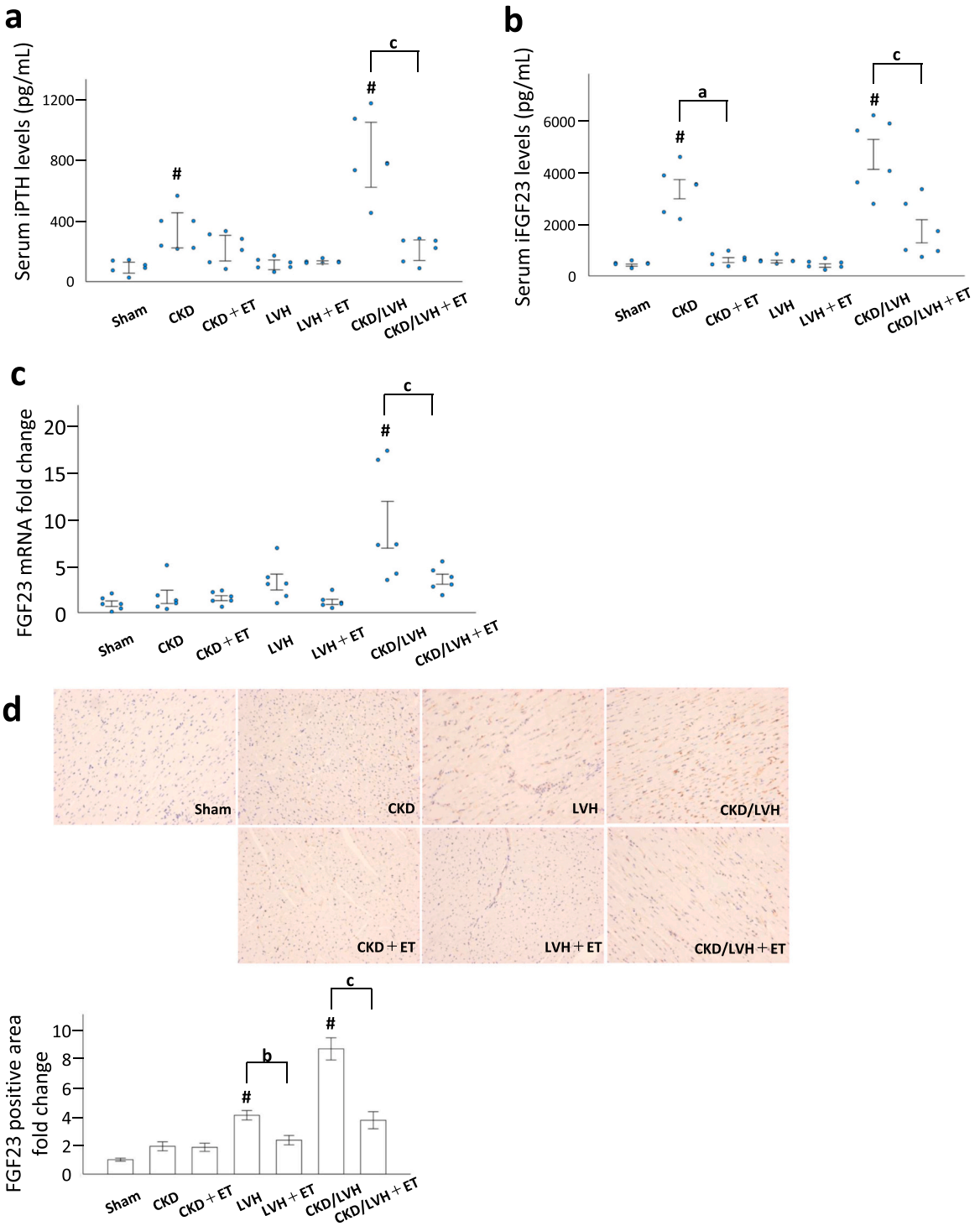

Fig. 4. Evaluation of serum intact parathyroid hormone (iPTH), and intact fibroblast growth factor 23 (iFGF23) in serum and heart tissue. (a) Serum levels of intact parathyroid hormone (iPTH). (b) Serum levels of intact fibroblast growth factor 23 (iFGF23). (c) Cardiac mRNA expression of FGF23. (d) Cardiac FGF23 expression evaluated by immunohistochemical staining. Data are presented as the mean ± SEM. #: $P < 0.05$ vs. Sham group; a: $P < 0.05$, CKD group vs. CKD + etelcalcetide (ET) group; b: $P < 0.05$, LVH group vs. LVH + ET group; c: $P < 0.05$, CKD/LVH group vs. CKD/LVH + ET group.

groups (Fig. 7d). Additionally, in the CKD/LVH group, the mRNA expression of cardiac AT1R was also significantly elevated, and it tended to decreased with ET treatment (Fig. 7e). In contrast, the mRNA expression of cardiac ACE2 was significantly suppressed in the LVH and CKD/LVH groups, and ET significantly increased its expression (Fig. 7c). There were no significant differences in renin mRNA expression in all groups (Fig. 7f).

Protein expression in cardiac tissue, evaluated through immunohistochemical analyses, revealed that the expression levels of ACE and Ang II were significantly increased in CKD/LVH groups and significantly decreased following ET treatment in the LVH and CKD/LVH groups (Fig. 7g and h). Additionally, cardiac ACE2 expression was significantly reduced in the CKD, LVH, and CKD/LVH groups and ET treatment tended to increase its expression (Fig. 7i).

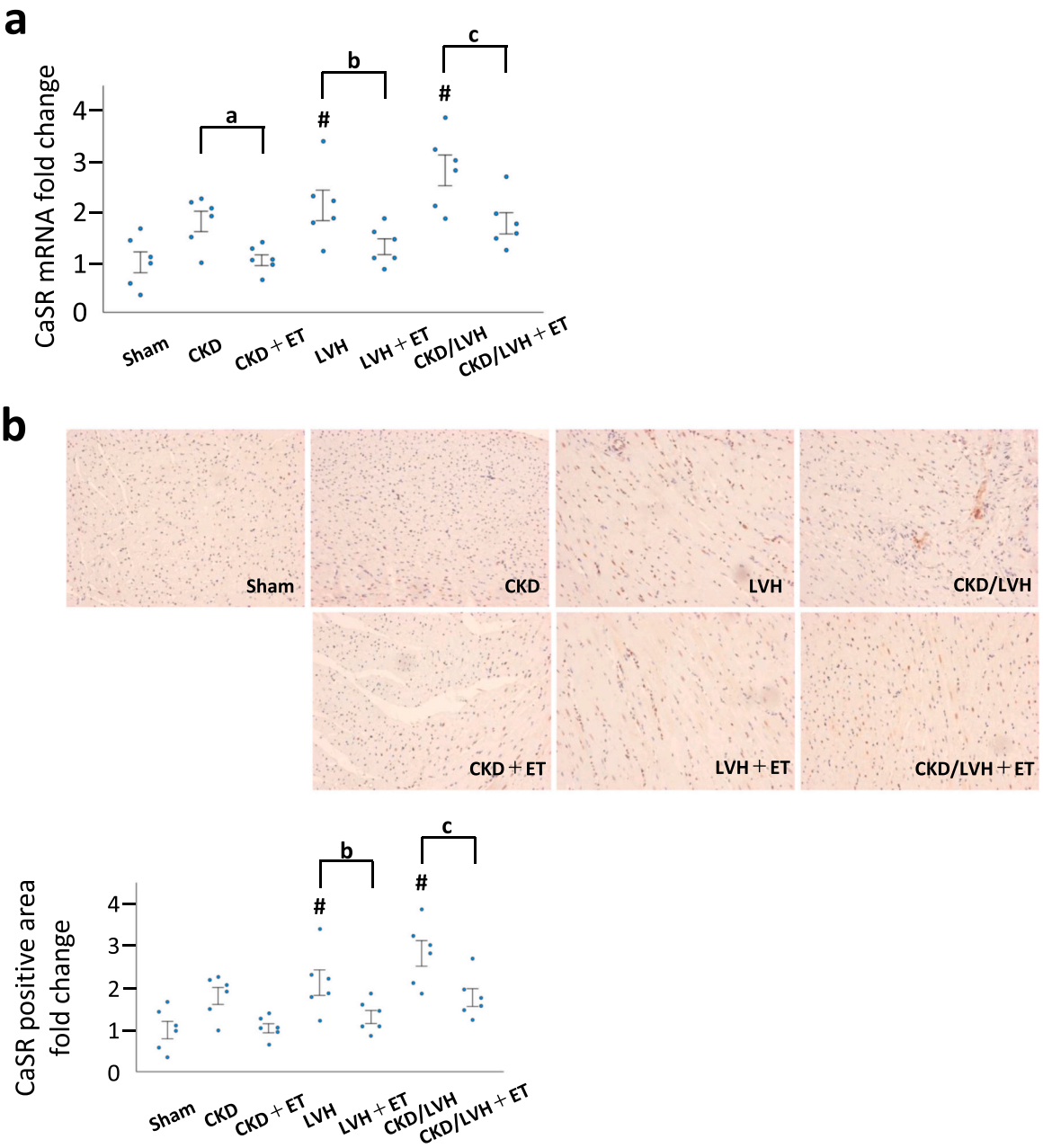

Fig. 5. Evaluation of calcium sensing receptor (CaSR) expression in the heart. (a) Cardiac mRNA expression of CaSR. (b) Cardiac CaSR expression evaluated by immunohistochemical staining. Data are presented as the mean ± SEM. #: $P < 0.05$ vs. Sham group; a: $P < 0.05$, CKD group vs. CKD + etelcalcetide (ET) group; b: $P < 0.05$, LVH group vs. LVH + ET group; c: $P < 0.05$, CKD/LVH group vs. CKD/LVH + ET group.

3.7. Systemic and cardiac oxidative stress

Urinary 8-OHdG levels, a marker of systemic oxidative stress, were elevated in the LVH and CKD/LVH groups, with the highest levels observed in the CKD/LVH group. ET significantly reduced urinary 8-OHdG levels in all groups (Fig. 8a). Local oxidative stress in myocardial tissue was assessed using immunohistochemical analyses. Oxidative stress was elevated in the CKD, LVH, and CKD/LVH groups, with the CKD/LVH group showing the most pronounced increase, consistent with the urinary 8-OHdG results (Fig. 8b). ET treatment alleviated systemic and cardiac oxidative stress across all groups.

4. Discussion

This study demonstrated that 1) ET improved LVH regardless of the presence of CKD; 2) ET suppressed RAAS elevations in the circulation and cardiac tissue in the LVH and CKD/LVH groups; 3) cardiac CaSR expression was upregulated in the LVH and CKD/LVH groups, and this upregulation was attenuated by ET administration; 4) although the CaN–NFAT pathway was activated in the LVH and CKD/LVH groups, ET treatment did not affect this activation; 5) oxidative stress was suppressed by ET administration in the CKD, LVH, and CKD/LVH groups.

Calcimimetics are widely used as therapeutic agents for hyperparathyroidism and are known to reduce serum PTH and FGF23 levels [21,26]. PTH and FGF23 are both considered key factors involved in LVH progression [27]. Clinical studies have reported a correlation between elevated PTH levels and increased left ventricular mass [9]. In basic research using mouse models, PTH administration has been shown to exacerbate cardiac hypertrophy and upregulate cardiac vascular endothelial growth factor and TGF-β1 expression, suggesting a possible role

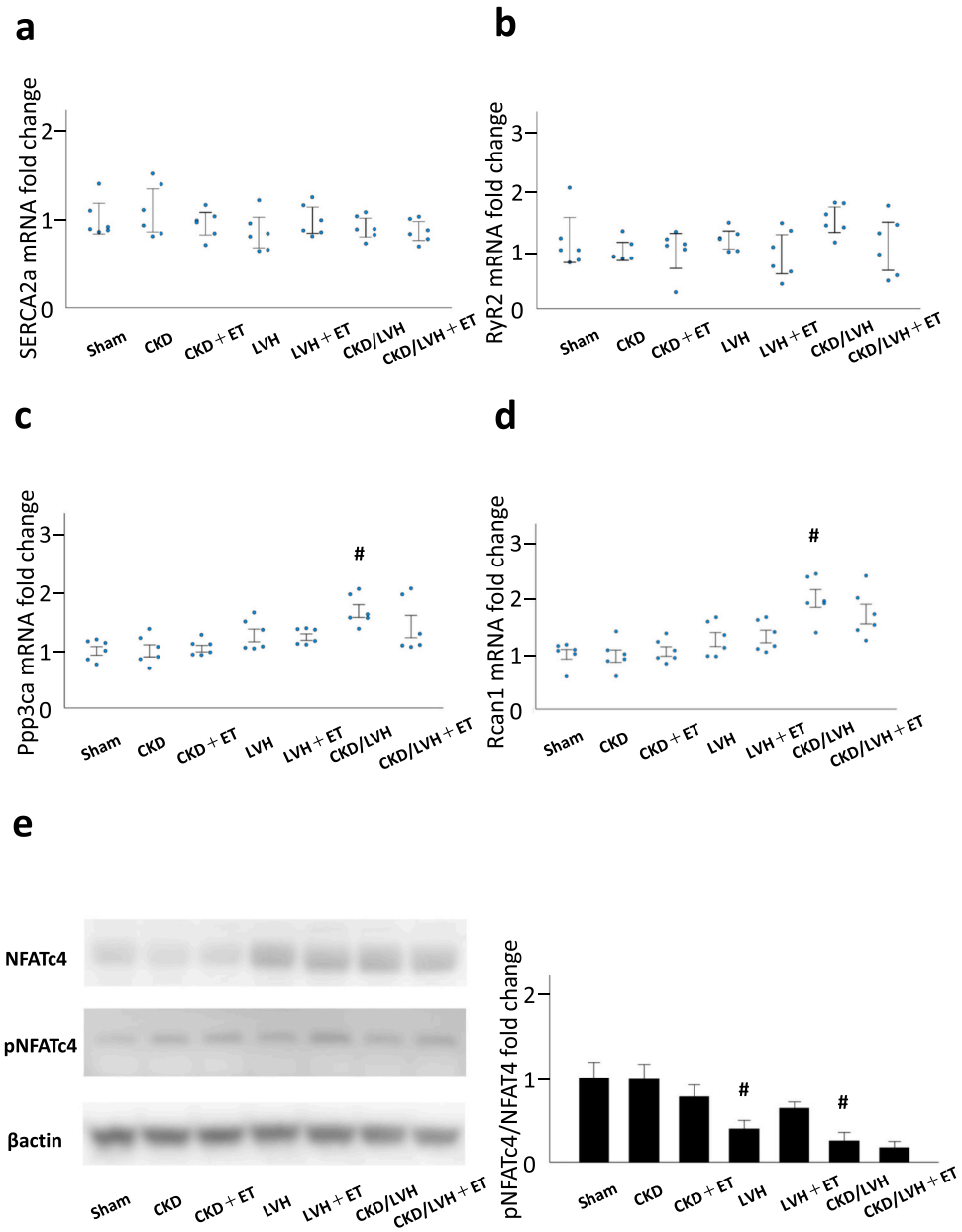

Fig. 6. Cardiac expression of factors related to intracellular calcium regulation and the calcineurin–nuclear factor of activated T cells (CaN–NFAT) signaling pathway. (a) Cardiac mRNA expression of sarcoplasmic/endoplasmic reticulum Ca^{2+} ATPase 2a (SERCA2a). (b) Cardiac mRNA expression of ryanodine receptor 2 (RyR2). (c) Cardiac mRNA expression of protein phosphatase 3 catalytic subunit alpha (Ppp3ca). (d) Cardiac mRNA expression of the regulator of calcineurin 1 (Rcan1). (e) Cardiac protein expression of the nuclear factor of activated T-cells 4 (NFATc4) and phosphorylated NFATc4 (p-NFATc4) by Western blot analysis. Data are presented as the mean ± SEM. #; $P < 0.05$, vs. sham group, a; $P < 0.05$, CKD group vs. CKD + etelcalcetide (ET) group, b; $P < 0.05$, LVH group vs. the LVH + ET group, c; $P < 0.05$, vs. the CKD/LVH group vs. CKD/LVH + ET group.

in LVH progression [28]. Similarly, elevated FGF23 levels have been demonstrated in clinical studies to be associated with LVH independently of traditional risk factors such as reduced eGFR, diabetes, and hypertension [12]. Moreover, in experimental models, FGF23 has been reported to activate the CaN–NFAT signaling pathway via FGF receptor 4, independently of klotho [13,29]. In the present study, ET administration led to reductions in serum PTH and FGF23 levels in the CKD and CKD/LVH groups. However, in the LVH group, these parameters remained unchanged despite a notable improvement in LVH. These findings suggest that while the antihypertrophic effects of ET may be partially mediated through the suppression of PTH and FGF23, the primary mechanisms likely involve other pathways.

In our study, cardiac hypertrophy progression was associated with increased cardiac CaSR expression, and this change was suppressed by ET. Previous studies have reported that cardiac CaSR expression is upregulated in response to hypertrophic stimuli such as Ang II or isoproterenol [30,31]. In addition, treatment with a CaSR antagonist (NPS 2143) has been shown to ameliorate cardiac hypertrophy and suppress the upregulation of cardiac CaSR expression [32]. These findings suggest that cardiac CaSR expression increases with cardiac hypertrophy progression and that ET may counteract this upregulation.

CaSR activation is known to increase intracellular calcium concentrations [33], which activates the CaN-NFAT signaling pathway [34]. Gadolinium (Gd^{3+}), a CaSR agonist, together with Ang II, induced greater cardiac hypertrophy compared to Ang II alone in rat cardiomyocytes, and this was associated with CaN-NFATc4 signaling pathway activation [35]. However, in our study, ET did not attenuate CaN-NFAT signaling pathway activation. While calcium is a well-known

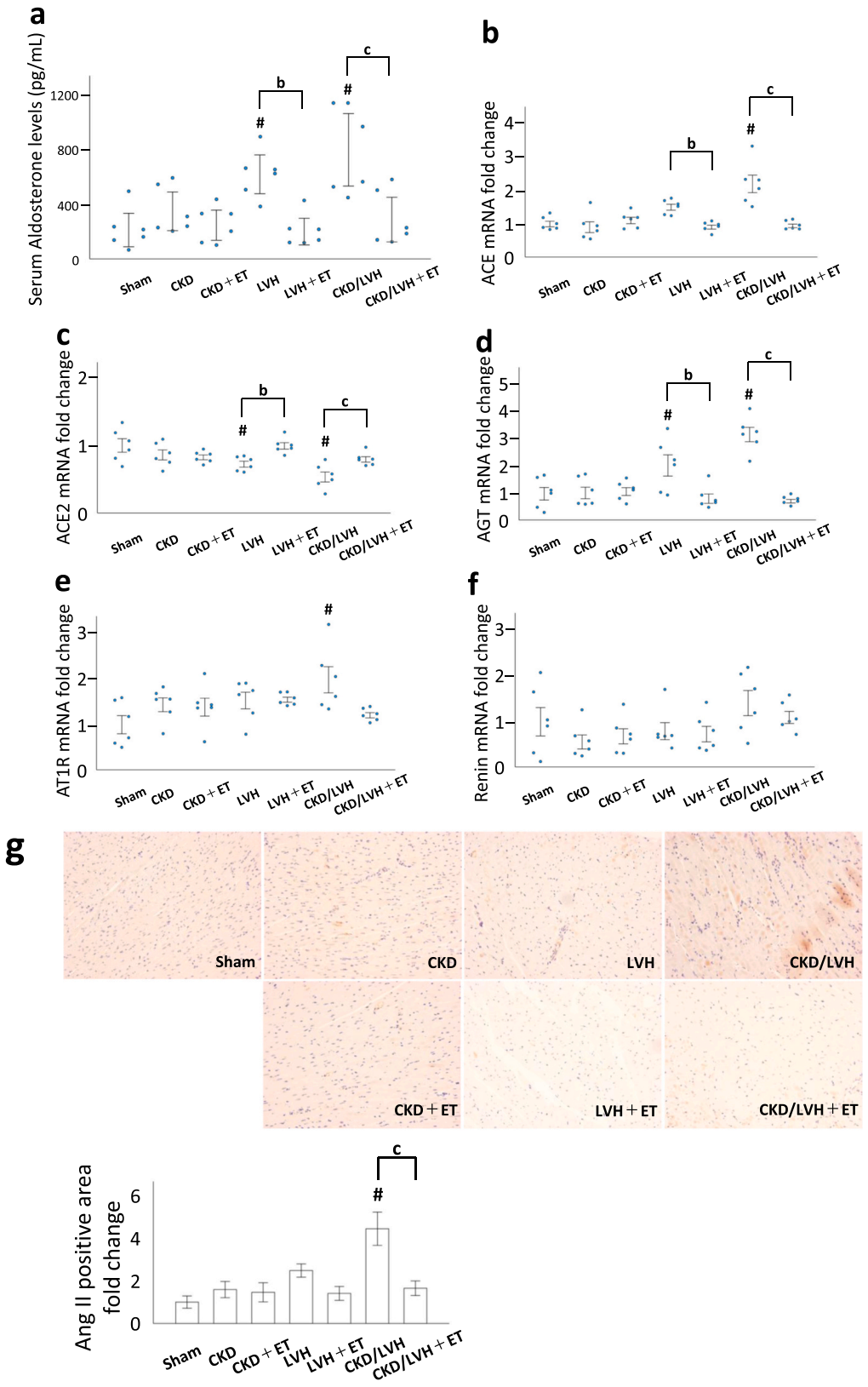

Fig. 7. Evaluation of serum aldosterone levels, cardiac mRNA expression of RAAS-related factors, and their expression by immunohistochemical staining in the heart. (a) Serum Aldosterone levels. (b) Cardiac mRNA expression of angiotensin-converting enzyme (ACE). (c) Cardiac mRNA expression of angiotensin-converting enzyme 2 (ACE2). (d) Cardiac mRNA expression of angiotensinogen (AGT). (e) Cardiac mRNA expression of angiotensin II type 1 receptor (AT1R). (f) Cardiac mRNA expression of Renin. (g) Cardiac protein expression of Angiotensin II (Ang II) by immunohistochemical staining. (h) Cardiac protein expression of ACE by immunohistochemical staining. (i) Cardiac protein expression of ACE2 by immunohistochemical staining. Data are presented as the mean ± SEM. #; $P < 0.05$, vs. sham group, a; $P < 0.05$, CKD group vs. CKD + etelcalcetide (ET) group, b; $P < 0.05$, LVH group vs. LVH + ET group, c; $P < 0.05$, vs. CKD/LVH group vs. CKD/LVH + ET group.

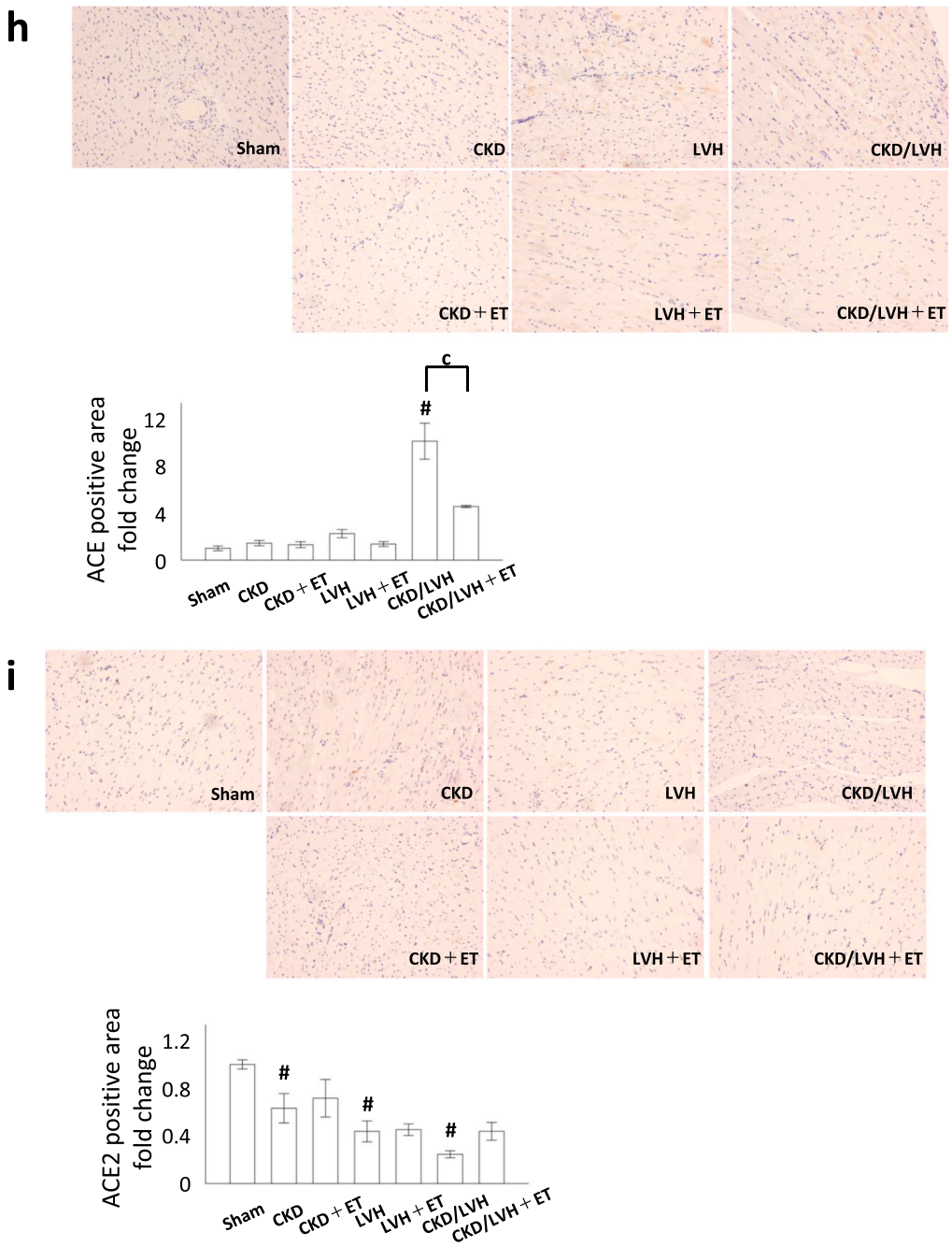

Fig. 7. (*continued*).

CaSR agonist, other agents such as phosphate, Gd^{3+}, and cadmium (Cd) are also known to activate CaSR, and it has been suggested that these agonists may differentially affect downstream signaling pathways [36]. Furthermore, previous studies have demonstrated that the CaSR agonist suppressed Cd-induced increments in intracellular calcium levels [37]. Additionally, a study using neonatal rat cardiomyocytes demonstrated that treatment with the calcimimetic AMG-073 under high Ca^{2+} conditions led to a decrease in ANP mRNA expression, suggesting a potential protective effect against cardiac hypertrophy [38]. Taken together, our findings suggest that etelcalcetide may suppress cardiac hypertrophy progression via other mechanisms independent of the CaN-NFAT signaling pathway in the heart.

The RAAS is a key contributor to cardiac hypertrophy progression [39,40]. Both basic and clinical studies have demonstrated that ACE inhibitors (ACE-Is) and Ang II receptor blockers improve cardiac hypertrophy [33,41]. Previous studies have reported that a CaSR agonist (R-568) ameliorated cardiac hypertrophy in hypertensive rats by reducing the expression of cardiac renin, AT1R, cyclic AMP (cAMP), and Ang II, while simultaneously increasing the expression of cardiac angiotensin (1−7) [Ang (1−7)] and angiotensin (1−9) [Ang (1−9)] [23]. Furthermore, R-568 administration in hypertensive rats was shown to suppress the expression of renin, Ang II, and AT1R in the thoracic aorta [42]. One proposed mechanism is that CaSR is expressed in the kidney, and calcimimetics may act on CaSR located in juxtaglomerular cells to inhibit renin secretion by suppressing adenylate cyclase and cAMP production [43].

Additionally, elevated levels of FGF23 and PTH have been associated with RAAS activation [44,45]. In the present study, although serum PTH and FGF23 levels were not elevated in the LVH group, cardiac FGF23 expression was increased, and this upregulation was suppressed by ET.

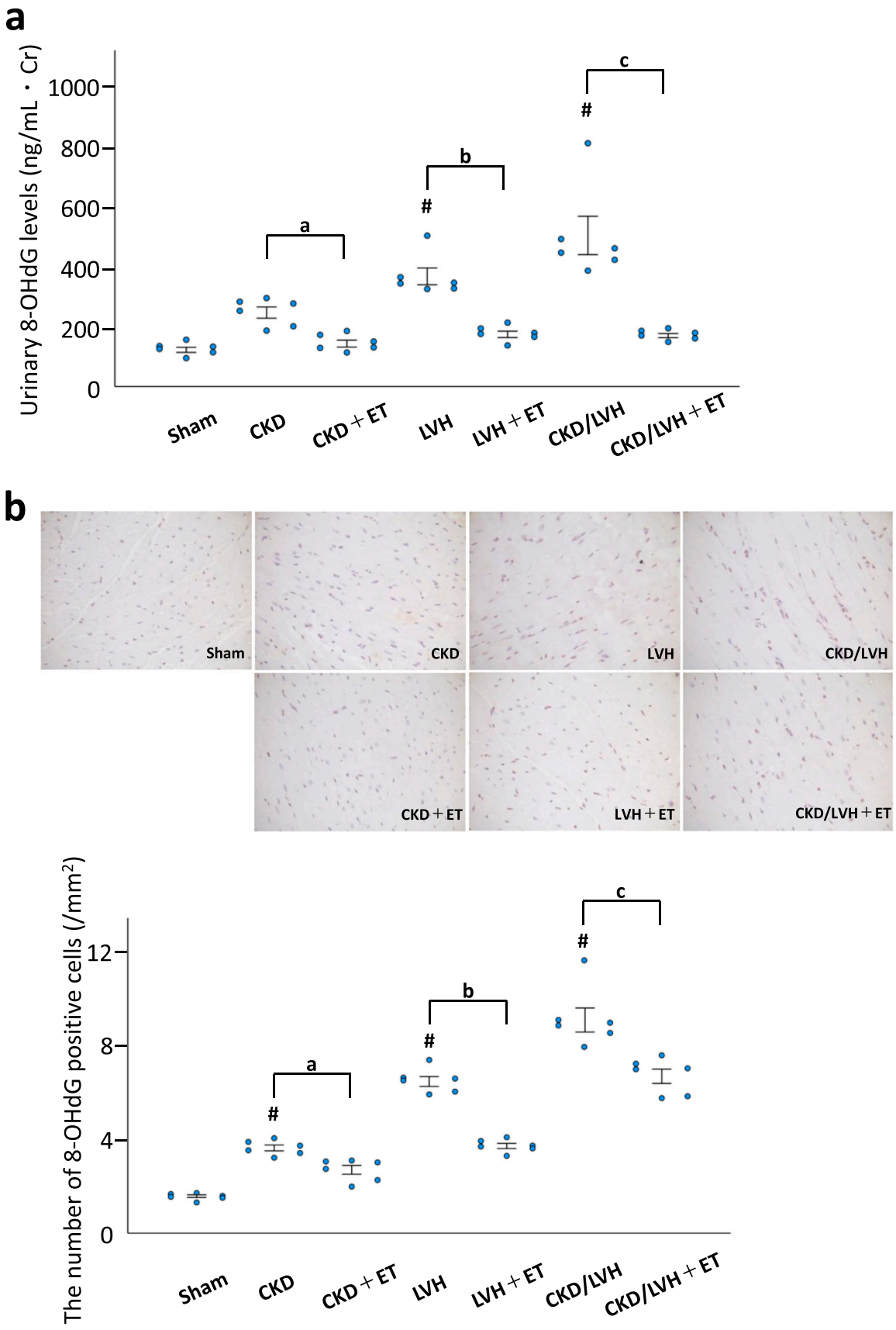

Fig. 8. Evaluation of oxidative stress. (a) Urinary 8-hydroxy-2′-deoxyguanosine (8-OHdG) levels. (b) Number of 8-OHdG-positive cells in the heart by immunohistochemical staining. Data are presented as the mean ± SEM. #; $P < 0.05$, vs. sham group, a; $P < 0.05$, CKD group vs. CKD + etelcalcetide (ET) group, b; $P < 0.05$, LVH group vs. LVH + ET group, c; $P < 0.05$, vs. CKD/LVH group vs. CKD/LVH + ET group.

Previous studies have demonstrated that in models of hypertension-induced and TAC-induced cardiac hypertrophy, FGF23 expression is significantly elevated in the myocardium itself rather than in bone. Although bone is an important site of FGF23 production, myocardial expression of FGF23 appears to be particularly relevant in the context of cardiac hypertrophy and fibrosis [46,47]. Moreover, have shown that Ang II and aldosterone suppress cardiac FGF23 expression [13,48], and that this effect is also inhibited by ACE-I in a mouse model of cardiac hypertrophy [49]. These findings suggest that RAAS contributes to the suppression of cardiac FGF23 expression. Collectively, the results indicate that calcimimetics may delay cardiac hypertrophy progression—at least in part—through RAAS inhibition.

Oxidative stress is also known to contribute to cardiac hypertrophy progression [50]. Previous studies have reported that calcimimetics reduce aortic levels of 8-OHdG in CKD rats [51] and lower circulating 8-OHdG levels in hemodialysis patients with secondary hyperparathyroidism [52]. In this study, we evaluated the urinary excretion and cardiac expression of 8-OHdG and observed a significant increase in oxidative stress associated with cardiac hypertrophy progression, which was suppressed by ET treatment. These findings suggest that the anti-hypertrophic effects of ET may, at least in part, be mediated through oxidative stress suppression.

This study has several limitations. First, we did not evaluate whether the effects of ET are independent of the CaN–NFAT signaling pathway, as experiments using CaN–NFAT transgenic rats were not performed. Second, the detailed mechanisms underlying the effects of ET, including its impact on the RAAS and other signaling pathways through CaSR, as well as intracellular Ca^{2+} dynamics in cardiomyocytes, remain unclear. Third, although Klotho is known to be involved in cardiac hypertrophy progression in CKD, its potential association was not assessed in this study.

5. Conclusion

ET suppressed cardiac hypertrophy progression in LVH and CKD/LVH rat models. This effect may be mediated through the suppression of the RAAS and oxidative stress.

CRediT authorship contribution statement

Shunsuke Goto: Supervision, Project administration. **Hidehisa Okamoto:** Writing – original draft, Visualization, Supervision, Investigation, Formal analysis, Data curation. **Yuma Nose:** Investigation. **Hideki Fujii:** Supervision, Project administration, Conceptualization. **Hayaki Okamoto:** Data curation.

Funding

None.

Declaration of Competing Interest

The authors declare the following financial interests/personal relationships which may be considered as potential competing interests: Hidehisa Okamoto reports equipment, drugs, or supplies was provided by Ono Pharmaceutical Co Ltd. Shunsuke Goto reports a relationship with Kyowa Kirin Co Ltd that includes: funding grants. Shunsuke Goto reports a relationship with Kyowa Kirin Co Ltd that includes: speaking and lecture fees. Shunsuke Goto reports a relationship with Sanwa Kagaku Kenkyusho Co Ltd that includes: speaking and lecture fees. Shunsuke Goto reports a relationship with Kissei Pharmaceutical Co Ltd that includes: speaking and lecture fees. Shunsuke Goto reports a relationship with Ono Pharmaceutical Co Ltd that includes: speaking and lecture fees. Hideki Fujii reports a relationship with Kyowa Kirin Co Ltd that includes: funding grants. Hideki Fujii reports a relationship with Kyowa Kirin Co Ltd that includes: speaking and lecture fees. Hideki Fujii reports a relationship with Sanwa Kagaku Kenkyusho Co Ltd that includes: speaking and lecture fees. Hideki Fujii reports a relationship with Kissei Pharmaceutical Co Ltd that includes: speaking and lecture fees. Hideki Fujii reports a relationship with Ono Pharmaceutical Co Ltd that includes: speaking and lecture fees. If there are other authors, they declare that they have no known competing financial interests or personal relationships that could have appeared to influence the work reported in this paper.

Acknowledgments

We received ET for this study from Ono Pharmaceutical Co., Ltd. This work was presented in part at the 2023 annual meeting of the European Renal Association.

Data availability

Data will be made available on request.

References

[1] R.T. Gansevoort, R. Correa-Rotter, B.R. Hemmelgarn, T.H. Jafar, H.J. Heerspink, J. F. Mann, et al., Chronic kidney disease and cardiovascular risk: epidemiology, mechanisms, and prevention, Lancet 382 (9889) (2013) 339, 52.
[2] D.E. Weiner, H. Tighiouart, P.T. Vlagopoulos, J.L. Griffith, D.N. Salem, A.S. Levey, et al., Effects of anemia and left ventricular hypertrophy on cardiovascular disease in patients with chronic kidney disease, J. Am. Soc. Nephrol. 16 (6) (2005) 1803, 10.
[3] D. Levy, R.J. Garrison, D.D. Savage, W.B. Kannel, W.P. Castelli, Prognostic implications of echocardiographically determined left ventricular mass in the Framingham Heart Study, N. Engl. J. Med 322 (22) (1990) 1561, 6.
[4] J.P. Law, L. Pickup, D. Pavlovic, J.N. Townend, C.J. Ferro, Hypertension and cardiomyopathy associated with chronic kidney disease: epidemiology, pathogenesis and treatment considerations, J. Hum. Hypertens. 37 (1) (2023) 1–19.
[5] E. Paoletti, D. Bellino, P. Cassottana, D. Rolla, G. Cannella, Left ventricular hypertrophy in nondiabetic predialysis CKD, Am. J. Kidney Dis. 46 (2) (2005) 320, 7.
[6] J.S. Silberberg, P.E. Barre, S.S. Prichard, A.D. Sniderman, Impact of left ventricular hypertrophy on survival in end-stage renal disease, Kidney Int 36 (2) (1989) 286, 90.
[7] G. Cerasola, E. Nardi, A. Palermo, G. Mulè, S. Cottone, Epidemiology and pathophysiology of left ventricular abnormalities in chronic kidney disease: a review, J. Nephrol. 24 (1) (2011) 1–10.
[8] S. Yamada, C.M. Giachelli, Vascular calcification in CKD-MBD: roles for phosphate, FGF23, and Klotho, Bone 100 (2017) 87–93.
[9] Saleh F.N. Schirmer, H. Sundsfjord, J. Jorde, R. Parathyroid hormone and left ventricular hypertrophy, Eur. Heart J. 24 (22) (2003) 2054, 60.
[10] L. Martínez-Arias, S. Panizo-García, J. Martín-Vírgala, B. Martín-Carro, S. Fernández-Villabrille, N. Avello-Llano, et al., Contribution of phosphorus and PTH to the development of cardiac hypertrophy and fibrosis in an experimental model of chronic renal failure, Nefrol. (Engl. Ed.) 41 (6) (2021) 640–651. Nov–Dec.
[11] P. Strózecki, A. Adamowicz, E. Nartowicz, G. Odrowaz-Sypniewska, Z. Włodarczyk, J. Manitius, Parathormon, calcium, phosphorus, and left ventricular structure and function in normotensive hemodialysis patients, Ren. Fail 23 (1) (2001) 115, 26.
[12] O.M. Gutiérrez, J.L. Januzzi, T. Isakova, K. Laliberte, K. Smith, G. Collerone, et al., Fibroblast growth factor 23 and left ventricular hypertrophy in chronic kidney disease, Circulation 119 (19) (2009) 2545, 52.
[13] C. Faul, A.P. Amaral, B. Oskouei, M.C. Hu, A. Sloan, T. Isakova, et al., FGF23 induces left ventricular hypertrophy, J. Clin. Invest 121 (11) (2011) 4393, 408.
[14] K. Yang, C. Wang, L. Nie, X. Zhao, J. Gu, X. Guan, et al., Klotho protects against indoxyl sulphate-induced myocardial hypertrophy, J. Am. Soc. Nephrol. 26 (10) (2015) 2434, 46.
[15] G.M. London, B. Pannier, A.P. Guerin, J. Blacher, S.J. Marchais, B. Darne, et al., Alterations of left ventricular hypertrophy in and survival of patients receiving hemodialysis: follow-up of an interventional study, J. Am. Soc. Nephrol. 12 (12) (2001) 2759, 67.
[16] J. Kong, G.H. Kim, M. Wei, T. Sun, G. Li, S.Q. Liu, et al., Therapeutic effects of vitamin D analogs on cardiac hypertrophy in spontaneously hypertensive rats, Am. J. Pathol. 177 (2) (2010) 622, 31.
[17] N. Bodyak, J.C. Ayus, S. Achinger, V. Shivalingappa, Q. Ke, Y.S. Chen, et al., Activated vitamin D attenuates left ventricular abnormalities induced by dietary sodium in Dahl salt-sensitive animals, Proc. Natl. Acad. Sci. USA 104 (43) (2007) 16810, 5.
[18] C.W. Park, Y.S. Oh, Y.S. Shin, C.M. Kim, Y.S. Kim, S.Y. Kim, et al., Intravenous calcitriol regresses myocardial hypertrophy in hemodialysis patients with secondary hyperparathyroidism, Am. J. Kidney Dis. 33 (1) (1999) 73–81.
[19] R. Thadhani, E. Appelbaum, Y. Pritchett, Y. Chang, J. Wenger, H. Tamez, et al., Vitamin D therapy and cardiac structure and function in patients with chronic

kidney disease: the PRIMO randomized controlled trial, JAMA 307 (7) (2012) 674, 84.
[20] A.Y. Wang, F. Fang, J. Chan, Y.Y. Wen, S. Qing, I.H. Chan, et al., Effect of paricalcitol on left ventricular mass and function in CKD–the OPERA trial, J. Am. Soc. Nephrol. 25 (1) (2014) 175, 86.
[21] S.M. Moe, G.M. Chertow, P.S. Parfrey, Y. Kubo, G.A. Block, R. Correa-Rotter, et al., Cinacalcet, fibroblast growth factor-23, and cardiovascular disease in hemodialysis: the evaluation of cinacalcet hcl therapy to lower cardiovascular events (EVOLVE) trial, Circulation 132 (1) (2015) 27–39.
[22] K. Dörr, M. Kammer, R. Reindl-Schwaighofer, M. Lorenz, T. Prikoszovich, R. Marculescu, et al., Randomized trial of etelcalcetide for cardiac hypertrophy in hemodialysis, Circ. Res 128 (11) (2021) 1616, 25.
[23] T. Zhang, N. Tang, D. Xi, Y. Zhao, Y. Liu, L. Wang, et al., Calcimimetic R568 improved cardiac remodeling by classic and novel renin-angiotensin system in spontaneously hypertensive rats, Exp. Biol. Med. (Maywood) 244 (10) (2019) 789–801.
[24] G.M. Chertow, G.A. Block, R. Correa-Rotter, T.B. Drüeke, J. Floege, W. G. Goodman, et al., Effect of cinacalcet on cardiovascular disease in patients undergoing dialysis, N. Engl. J. Med. 367 (26) (2012) 2482, 94.
[25] J.C. McGrath, E. Lilley, Implementing guidelines on reporting research using animals (ARRIVE etc.): new requirements for publication in BJP, Br. J. Pharm. 172 (13) (2015) 3189, 93.
[26] G.A. Block, D.A. Bushinsky, S. Cheng, J. Cunningham, B. Dehmel, T.B. Drueke, et al., Effect of etelcalcetide vs cinacalcet on serum parathyroid hormone in patients receiving hemodialysis with secondary hyperparathyroidism: a randomized clinical trial, JAMA 317 (2) (2017) 156, 64.
[27] J.A. Navarro-García, M. Fernández-Velasco, C. Delgado, J.F. Delgado, M. Kuro-O, L.M. Ruilope, et al., PTH, vitamin D, and the FGF-23-klotho axis and heart: Going beyond the confines of nephrology, Eur. J. Clin. Invest 48 (4) (2018).
[28] H. Cha, H.J. Jeong, S.P. Jang, J.Y. Kim, D.K. Yang, J.G. Oh, et al., Parathyroid hormone accelerates decompensation following left ventricular hypertrophy, Exp. Mol. Med 42 (1) (2010) 61, 8.
[29] A. Grabner, A.P. Amaral, K. Schramm, S. Singh, A. Sloan, C. Yanucil, et al., Activation of cardiac fibroblast growth factor receptor 4 causes left ventricular hypertrophy, Cell Metab. 22 (6) (2015) 1020, 32.
[30] J. Chi, L. Wang, X. Zhang, Y. Fu, Y. Liu, W. Chen, et al., Activation of calcium-sensing receptor-mediated autophagy in angiotensinII-induced cardiac fibrosis in vitro, Biochem Biophys. Res. Commun. 497 (2) (2018) 571, 6.
[31] L. Liu, C. Wang, Y. Lin, Y. Xi, H. Li, S. Shi, et al., Suppression of calcium-sensing receptor ameliorates cardiac hypertrophy through inhibition of autophagy, Mol. Med. Rep. 14 (1) (2016) 111, 20.
[32] M.L. Lu, J. Wang, Y. Sun, C. Li, T.R. Sun, X.W. Hou, et al., Ginsenoside Rg1 attenuates mechanical stress-induced cardiac injury via calcium sensing receptor-related pathway, J. Ginseng Res. 45 (6) (2021) 683, 94.
[33] J.R. Paull, R.E. Widdop, Persistent cardiovascular effects of chronic renin-angiotensin system inhibition following withdrawal in adult spontaneously hypertensive rats, J. Hypertens. 19 (8) (2001) 1393, 402.
[34] J.D. Molkentin, J.R. Lu, C.L. Antos, B. Markham, J. Richardson, J. Robbins, et al., A calcineurin-dependent transcriptional pathway for cardiac hypertrophy, Cell 93 (2) (1998) 215, 28.
[35] L.N. Wang, C. Wang, Y. Lin, Y.H. Xi, W.H. Zhang, Y.J. Zhao, et al., Involvement of calcium-sensing receptor in cardiac hypertrophy-induced by angiotensinII through calcineurin pathway in cultured neonatal rat cardiomyocytes, Biochem Biophys. Res. Commun. 369 (2) (2008) 584, 9.
[36] A.R. Thomsen, M. Hvidtfeldt, H. Bräuner-Osborne, Biased agonism of the calcium-sensing receptor, Cell Calcium 51 (2) (2012) 107, 16.
[37] J. Gu, S. Dai, Y. Liu, H. Liu, Y. Zhang, X. Ji, et al., Activation of Ca^{2+}-sensing receptor as a protective pathway to reduce Cadmium-induced cytotoxicity in renal proximal tubular cells, Sci. Rep. 8 (1) (2018) 1092.
[38] R. Jabbari, S. Smajilovic, N. Chattopadhyay, S. Haunso, J. Tfelt-Hansen, The Calcium-Sensing Receptor is Upregulated in Post Myocardial Infarct Hearts and Downregulates ANP Expression in Rat Cardiac Myocytes but is Not Expressed in Rat Cardiac Fibroblasts In Vitro, Open Endocrinol. J. 5 (2011) 1, 7.
[39] D.V. Vlahakos, G. Hahalis, P. Vassilakos, K.P. Marathias, S. Geroulanos, Relationship between left ventricular hypertrophy and plasma renin activity in chronic hemodialysis patients, J. Am. Soc. Nephrol. 8 (11) (1997) 1764, 70.
[40] B.R. Cowan, A.A. Young, Left ventricular hypertrophy and renin-angiotensin system blockade, Curr. Hypertens. Rep. 11 (3) (2009) 167, 72.
[41] R.H. Fagard, H. Celis, L. Thijs, S. Wouters, Regression of left ventricular mass by antihypertensive treatment: a meta-analysis of randomized comparative studies, Hypertension 54 (5) (2009) 1084, 91.
[42] R. Sun, W. Zhang, H. Zhong, L. Wang, N. Tang, Y. Liu, et al., Calcimimetic R568 reduced the blood pressure and improved aortic remodeling in spontaneously hypertensive rats by inhibiting local renin-angiotensin system activity, Exp. Ther. Med 16 (5) (2018) 4089, 99.
[43] D.K. Atchison, M.C. Ortiz-Capisano, W.H. Beierwaltes, Acute activation of the calcium-sensing receptor inhibits plasma renin activity in vivo, Am. J. Physiol. Regul. Integr. Comp. Physiol. 299 (4) (2010) R1020, 6.
[44] B. Dai, V. David, A. Martin, J. Huang, H. Li, Y. Jiao, et al., A comparative transcriptome analysis identifying FGF23 regulated genes in the kidney of a mouse CKD model, PLoS One 7 (9) (2012) e44161.
[45] M.H. Zheng, F.X. Li, F. Xu, X. Lin, Y. Wang, Q.S. Xu, et al., The interplay between the renin-angiotensin-aldosterone system and parathyroid hormone, Front. Endocrinol. 11 (2020) 539.
[46] H. Fujii, K. Watanabe, K. Kono, S. Goto, S. Watanabe, S. Nishi, Changes in serum and intracardiac fibroblast growth factor 23 during the progression of left ventricular hypertrophy in hypertensive model rats, Clin. Exp. Nephrol. 23 (5) (2019) 589, 96.
[47] S. Slavic, K. Ford, M. Modert, A. Becirovic, S. Handschuh, A. Baierl, et al., Genetic Ablation of Fgf23 or Klotho Does not Modulate Experimental Heart Hypertrophy Induced by Pressure Overload, Sci. Rep. 7 (1) (2017) 11298.
[48] M. Leifheit-Nestler, F. Kirchhoff, J. Nespor, B. Richter, B. Soetje, M. Klintschar, et al., Fibroblast growth factor 23 is induced by an activated renin-angiotensin-aldosterone system in cardiac myocytes and promotes the pro-fibrotic crosstalk between cardiac myocytes and fibroblasts, Nephrol. Dial. Transpl. 33 (10) (2018) 1722, 34.
[49] K. Watanabe, H. Fujii, K. Okamoto, K. Kono, S. Goto, S. Nishi, Exploring the implications of blocking renin-angiotensin-aldosterone system and fibroblast growth factor 23 in early left ventricular hypertrophy without chronic kidney disease, Front. Endocrinol. 14 (2023) 1276664.
[50] A.K. Shah, S.K. Bhullar, V. Elimban, N.S. Dhalla, Oxidative stress as a mechanism for functional alterations in cardiac hypertrophy and heart failure, Antioxidants 10 (6) (2021).
[51] J.G. Damrath, N.X. Chen, C.E. Metzger, S. Srinivasan, K. O'Neill, A. Biruete, et al., Non-additive effects of combined nox1/4 inhibition and calcimimetic treatment on a rat model of chronic kidney disease-mineral and bone disorder (CKD-MBD), JBMR 6 (3) (2022) e10600.
[52] E. Ari, Y. Kaya, H. Demir, E. Asicioglu, Z. Eren, E. Celik, et al., Cinacalcet may improve oxidative DNA damage in maintenance hemodialysis patients: an observational study, Int Urol. Nephrol. 46 (9) (2014) 1843, 9.